X-point effect on edge stability

S. Saarelma[1], O.J. Kwon[2], A. Kirk[1] and MAST Team

[1] EURATOM/CCFE Fusion Association, Culham Science Centre, Abingdon, OX14 3DB, UK

[2] Dept. Of Physics, Daegu University, Gyungbuk, Korea

E-mail: samuli.saarelma@ccfe.ac.uk

Abstract. We study the effects of the X-point configuration on ELM triggering peeling and ballooning modes by using fixed boundary equilibria and modifying the plasma shape to approach the limit of a true X-point. The current driven pure peeling modes are asymptotically stabilised by the X-point while the stabilising effect on ballooning modes depends on the poloidal location of the X-point. The coupled peeling-ballooning modes experience the elimination of the peeling component as the X-point is introduced. This can significantly affect the edge stability diagrams used to analyse the ELM triggering mechanisms.

PACS numbers: 52.55.Fa

Submitted to: *Plasma Physics and Controlled Fusion*

1. Introduction

The edge plasma stability plays an important role in the modern tokamak operations due to the ELM (Edge Localised Mode) phenomenon. Most tokamaks operate in a diverted configuration with an X-point where the poloidal field vanishes and a separatrix separating the closed flux surface region from the open field lines. As the ELMs are most likely instabilities localised near the plasma edge [1], the X-point configuration can potentially affect any ELM simulations. The separatrix with an X-point poses an especially difficult problem for most ideal MHD stability codes that use straight field line coordinates because the grid points become strongly packed near the X-point on surfaces close to the separatrix, but not on surfaces deeper inside the plasma.

The ELMs are believed to be triggered by a combination of current driven peeling and pressure driven ballooning modes[1, 2]. X-point effects on peeling mode stability with zero edge current (mode driven by the finite current gradient) were studied by Huysmans using CASTOR [3] and found to be strongly stabilising, though with finite edge current little effect was found[3].

In this paper we approach the true X-point configuration asymptotically by starting from an ellipse shaped plasma cross-section and introducing a small local perturbation to the shape. As we increase the perturbation, the field lines at the plasma edge spend more time near the perturbation just like they do near a true X-point. The q-profile and especially the shear increase near the edge which is also similar to the effect of an X-point. We investigate how the location of the X-point affects the peeling and ballooning modes and how the stability diagrams used to determine the ELM triggering instability are modified by the X-point effects.

2. Equilibrium

Since our aim is to study the effect of an X-point on the edge MHD instabilities, we isolate all the other effects from the equilibrium that could affect the stability. As a reference we use an equilibrium that has an ellipse as the poloidal cross-section. As discussed in [4], it is possible to modify the shape of a plasma's edge with an arbitrarily small, poloidally and radially localised perturbation. The shape of the unperturbed and perturbed plasma are shown in Fig. 1. All the equilibria considered in this study are up-down symmetric. The perturbation that introduces a very sharp bend in the edge acts as an X-point. To produce an equilibrium with such a sharp bend the poloidal field must become very small in the vicinity of the perturbation. This in turn increases the safety factor q and especially the magnetic shear $s = dq/dr\ r/q$ as is shown in Fig. 2 where the edge q and s profiles are plotted for the two shapes in Fig. 1. In the studies of the X-point's poloidal location effect on stability we vary its angle θ, defined in Fig. 1.

It must be noted that even though magnetic shear has increased by almost two orders of magnitude with the introduction of the perturbation, the q at the plasma edge

has only increased from 3.9 to 4.2. This means that the rational surfaces inside the plasma have hardly changed and, thus, the potential changes in stability are unlikely to be due to changes in mode numbers.

We choose the current and pressure profiles so that the reference case is unstable against peeling and ballooning modes. For peeling modes the edge pressure gradient vanishes, but there is finite current at the plasma edge. For ballooning modes, the edge current vanishes, but there is a steep pressure gradient near the edge. For the combined peeling-ballooning modes we use the ballooning mode pressure profile and a current profile that has a peak near the edge representing the bootstrap current driven by the pressure gradient. The profiles are shown in Fig. 3.

We solve the ideal MHD equilibrium using the HELENA code[5]. To achieve sufficient resolution near the edge, we use strong packing. For the entire equilibrium we use 300 radial and 1025 poloidal points and of the radial points, 100 are used in the last 0.5% of the poloidal flux. Since HELENA uses straight field line coordinates, the poloidal points are packed automatically in the region of low poloidal magnetic field, i.e. near the X-point.

3. Stability Changes due to X-point

We study the stability of the constructed equilibria using the ELITE code[6, 7]. In the stability analysis we study two classes of instabilities that are thought to be relevant to ELMs, current driven peeling modes and pressure driven ballooning modes. The radial mode structure of these modes is shown in Fig. 4. The peeling mode is characterised by a single poloidal harmonic that peaks at the plasma edge while the ballooning mode has several poloidal harmonics and a wider radial extent.

3.1. Peeling Modes

First we study the effect of approaching the X-point shape by introducing the perturbation on the bottom (and top, since the plasma is up-down symmetric) of the plasma ($\theta = 0.5\pi$). We use magnetic shear as a measure of the "closeness" of the X-point configuration, i.e. the closer the plasma is to an actual X-point geometry the higher the magnetic shear. As was shown above, even though the safety factor q changes only little with the shaping, the edge shear is very sensitive to the closeness to an actual X-point configuration.

When plotted on a log-log scale the growth rate of the $n = 5$ pure peeling mode decreases linearly with shear as shown in Fig. 5. This means that the growth rate approaches zero asymptotically as the plasma shape approaches the X-point configuration. The relation between shear and growth rate is

$$\ln(\gamma) = 0.5 \ln(s) + C. \tag{1}$$

The numerical result matches with an analytical result for peeling modes in X-point plasmas by Webster et al.[8].

Next we study how the poloidal location of the X-point affects the stability. When we vary the angle θ from the $\pi/2$ value that was used above, we find that the stabilising effect of the X-point on peeling modes is not affected significantly by the location of the X-point. As Fig. 6 shows, the growth rate of the peeling mode only depends on the sharpness of the X-point that is characterized by the magnetic shear at the plasma edge and not on the poloidal location. This agrees with the result in [3].

3.2. Ballooning Modes

The local analysis for $n = \infty$ ballooning modes by Bishop et al. showed that locating the X-point on the high field side is the most favourable for stability [9, 10]. He showed that the picture of ballooning stability in X-point plasmas is complicated. On one hand the connection length between high inside and outside of the torus increases due to the low poloidal field near the X-point. This weakens the stability. On the other hand, if the X-point is on the inside of the torus, the stability is improved because the field line lingers for much of its length on the good curvature ($< \kappa \cdot \nabla p >< 0$) side of the plasma. An X-point on the outside of the torus has the opposite effect degrading the stability.

We study here the stability of $n = 20$ ballooning modes with finite eigenfunction width. The growth rate of these modes as a function poloidal location of the X-point is shown in Fig. 7 for several values of edge shear (X-point "sharpness"). If the X-point is on the top of the plasma ($\theta = 0.5\pi$), the mode fully stabilises as the X-point is sharpened. This full stabilisation is not necessarily a universal property, but only applies with the given profiles due to plasma being relatively close to the marginal stability. If the X-point is located in the high field side of the plasma ($\theta = 0.7\pi$), the growth rate of the ballooning mode first decreases and then saturates as the X-point becomes sharper. This is due to the fact that the ballooning mode is localised on the low field side of the plasma. Consequently, any improvement in stability on the high field side has little effect. However, the X-point on the low field side ($\theta = 0.3\pi$) has a strongly destablising effect on the mode. Only a modest increase in shear causes a large increase in growth rate. The X-point makes field lines more concentrated on the unfavourable low field side, which greatly increases the drive of the ballooning mode. Note that Figure 7 is missing high shear points for the low field side located X-point. This is due to the fact that in these cases the ELITE code no longer converges.

From the ballooning mode stability point of view, the optimal location for the X-point is around the top (or bottom) of the plasma. This supports the view of [4], that perturbing the plasma towards an X-point on the outboard side might provide a tunable means for controlling the edge pressure gradient - a sharper perturbation leading to a reduced edge pressure. The result for the low field side X-point agrees with a similar study for TCV plasmas [11]. In that study it was also found that a low-field side X-point strongly destabilises the ballooning modes.

3.3. Combined Peeling-Ballooning Modes

In most experimental plasmas the edge stability is not actually constrained by pure peeling or ballooning modes, but by a combination of these two. Several studies for various tokamaks have found the edge of Type I ELMy plasmas to be limited by intermediate-n peeling-ballooning modes [7, 12, 13]. Since the stability effect of the X-point is quite different for peeling and ballooning modes, we study separately the effect on modes that have both components present. In this study, the X-point is localised on the top (and bottom) ($\theta = 0.5\pi$) of the plasma (as in the peeling mode study) to avoid the strong destabilising effect of the low-field side X-point on ballooning modes. This is also the most relevant location of the X-point with regards to current day tokamak experiments. The current and pressure profile used in this study are shown in Fig.3 and represent the typical shapes of an H-mode plasma. In addition to a steep edge pressure gradient, there is also a current peak near the edge that represents the bootstrap current.

As expected the sharpening of the X-point has an effect on the stability that combines the effects of peeling and ballooning mode studies. As was shown above, the peeling mode growth rate decreases with the sharpening X-point, but the ballooning stability can both improve or worsen. With the X-point on the top the net effect is that the ballooning component of the instability is not much affected while the peeling component is stabilised. This is shown in Fig. 8 where the growth rates of modes with varying toroidal mode number n are plotted against the edge shear. The peeling-ballooning modes with low n are like pure peeling modes. As n increases the combined peeling-ballooning becomes more ballooning mode like. Consequently, the growth rate of low-n modes follow the peeling mode behaviour, i.e. decreases logarithmically with edge magnetic shear. The growth rate of high-n modes first decreases with shear like that of low-n modes and then after a certain point is not affected by changes in the sharpness of the X-point. The decrease is due to the peeling component of the mode being stabilised. Unlike in the pure ballooning mode case, the high-n ballooning mode growth rate in the static case is higher. Therefore, the sharpening of the X-point does lead only a finite reduction of the growth rate instead of the full stabilisation. In the radial mode structure of the high-n modes in plasmas with a sharp X-point the peeling component has disappeared, while the ballooning part is hardly affected as shown in Fig. 9 where the radial mode structure of the n=20 mode with and without an X-point is plotted.

4. X-point Effect on Experimental MAST Plasma Edge Stability

Finally, we study how the stabilising effect of the X-point affects the stability boundaries of a realistic MAST plasma. The chosen plasma (#8209 at 0.3s) is a double null Type I ELMy plasma with global parameters of $I_p = 0.77$MA and $B_t = 0.56$T. More details of the experiment can be found in [14]. The pressure and toroidal current density profiles

are shown in Fig. 10. The electron pressure profile is derived from a fit to the high-resolution Thomson scattering diagnostic (300 horizontal points at mid-plane). The ion pressure is assumed to be equal to the electron pressure. The edge current is from a self-consistent bootstrap current calculation using formulas from Ref. [15, 16]. The two shapes that we test here are shown in Fig. 11. As can be seen, the X-point is slightly on the high field side. The shapes differ from each other only by the sharpness of the X-point. The value of the edge magnetic shear of the two shapes are 8.3 (round) and 18.3 (sharp).

We vary the edge pressure gradient and current density around the experimental point, create a new equilibrium and analyse its stability. This allows us to draw a diagram around the experimental equilibrium that shows the stability boundaries that limit the profiles in the experiment. Figure 12 shows the stability diagrams for plasma with sharp and round X-points. The numbers represent the most unstable mode. The definition of the normalised pressure gradient α used in the diagram is [17]:

$$\alpha = \frac{-2\partial V/\partial\psi}{(2\pi)^2}\left(\frac{V}{2\pi^2 R_0}\right)^{1/2}\mu_0\frac{\partial p}{\partial\psi}. \qquad (2)$$

Here V is the plasma volume enclosed in a flux surface with the poloidal flux value ψ, p is the pressure and R_0 is the geometric centre of the plasma.

While the stability boundary against high-n ballooning modes stays almost constant with the change of X-point sharpness, the low-n peeling and peeling-ballooning boundary is somewhat expanded towards higher edge current with the sharpening of the X-point. This agrees well with results presented above for model plasmas.

5. Conclusions

We have shown that the X-point can have a significant effect on the ELM triggering instabilities, especially peeling modes. The logarithm of the peeling mode growth rate decreases roughly linearly with the logarithm of the edge shear. The peeling part of the instability is even stabilised in a combined peeling-ballooning mode.

The strong stabilising effect of the X-point on peeling modes can strongly change the stability diagrams that are used to determine which modes are triggering ELMs. Since the growth rate of the pure peeling modes decreases asymptotically towards zero as the fixed boundary equilibrium approaches the actual X-point equilibrium, it seems unlikely that peeling modes can act as a trigger of an ELM in a diverted plasma especially if we assume as in [1] that the growth of the unstable mode has to overcome the diamagnetic stabilisation and the growth rate has to exceed a finite value e.g. $\omega^*/2$. However the ELM crash is a non-linear phenomenon. Therefore, the marginally stable peeling modes may still play a role in it. A non-linear analysis is required to determine whether or not this is the case. In addition as shown by Huysmanns, including the resistivity can restore a role for peeling modes as ELM triggers [3].

In addition to the stability diagrams, the X-point also modifies the mode structure of the ELM triggering peeling-ballooning instability by eliminating the edge peaking

peeling component and leaving only the ballooning structure that peaks inside the separatrix.

6. Acknowledgemet

This work was jointly funded by the United Kingdom Engineering and Physical Sciences Research Council under grant EP/G003955 and by the European Communities under the Contract of Association between EURATOM and CCFE. The views and opinions expressed herein do not necessarily reflect those of the European Commission. A visit of one of the authors (O.J. Kwon) to CCFE was supported by National R&D Program through the National Research Foundation of Korea(NRF) funded by the Ministry of Education, Science and Technology (No 2009-0082635).

[1] Snyder, P.B. et al., Phys. of Plasmas **9** (2002) 2037.
[2] Wilson, H.R., et al. Plasma Phys. Contr. Fusion **48** (2006) A71
[3] Huysmans G.T.A., Plasma Phys. Contr. Fusion, **47** (2005) 2107.
[4] Webster A.J., Phys. Plasmas **16** (2009) 012501.
[5] Huysmans G.T.A., Goedbloed J.P., Kerner W.O.K., Computational Physics (Proc. Int. Conf. Amsterdam, 1991),World Scientific Publishing, Singapore (1991) 371.
[6] Wilson H.R., Snyder P.B., Huysmans G.T.A. and Miller R.L., Phys. Plasmas **9** (2002) 1277.
[7] Snyder P.B., Wilson H.R., et al., Phys. Plasmas **9** (2002) 2037.
[8] Webster A.J., Gimblett C.G., Phys. Rev. Lett. **102** (2009) 035003.
[9] Bishop C.M., et al. Nucl. Fusion **24** (1984) 1579
[10] Bishop C.M., Nucl. Fusion **26** (1986) 1063
[11] Medvedev S. Yu., et al., Proceedings of 35th EPS Conf. on Controlled Fusion and Plasma Physics, Hersonissos, Greece, 2008.
[12] Maggi C.F., et al., Plasma Phys. Contr. Fusion **50** (2010) 025023.
[13] Saarelma S., et al. Plasma Phys. Contr. Fusion **49** (2009) 035001.
[14] Kirk. A. et al. Plasma Phys. Contr. Fusion **51** (2009) 065016.
[15] Sauter O., Angioni C., Lin-Liu Y.R., Phys. of Plasmas, **6** (1999) 2834.
[16] Sauter O., Angioni C., Lin-Liu Y.R., Phys. of Plasmas, **9** (2002) 5140.
[17] Miller R.L., et al., Phys. of Plasma **5** (1998) 973.

Figure captions

Figure 1. The shape of the last flux surface for the base case equilibrium (dashed line) and steep X-point equilibrium (solid line). The θ angle is used to vary the poloidal location of the X-point.

Figure 2. The radial q and magnetic shear profiles of the base case equilibrium (dashed line) and steep X-point equilibrium (solid line) near the plasma edge.

Figure 3. The normalised pressure and toroidal current profiles used for peeling and peeling-ballooning modes

Figure 4. The radial mode structure of $n = 5$ peeling mode (left) and $n = 20$ ballooning mode. X is the radial perturbation of the fluid element. The individual lines represent contributions of different poloidal mode numbers u_m, i.e. the total displacement is $\sum_m u_m(\psi)e^{-im\omega}$.

Figure 5. The growth rate of $n = 5$ peeling modes as a function of the edge shear (X-point "sharpness").

Figure 6. The growth rate of $n = 5$ peeling modes as a function of the edge shear (X-point "sharpness") for three poloidal locations of the X-point.

Figure 7. The growth rate of $n = 20$ ballooning mode as a function of the X-point poloidal location for four values of the edge shear.

Figure 8. The growth rate of peeling-ballooning modes as a function of the edge shear (X-point "sharpness").

Figure 9. The radial mode structure of n=20 peeling-ballooning mode without (left) and with X-point (right). The X-point case corresponds to the equilibrium with edge shear of 152 in Fig. 8

Figure 10. The plasma pressure and flux surface averaged toroidal current profile of MAST discharge #8209.

Figure 11. The plasma shape of MAST discharge #8209 with round (dashed line) and sharp (solid line) X-point.

Figure 12. The edge stability diagram for the two plasma shapes of a MAST discharge #8209. The colour represents the growth rate of the mode (dark blue=stable). The left diagram corresponds to a round X-point ($s_{edge} = 8.3$) and the right to a sharp X-point ($s_{edge} = 18.3$). The numbers represent the most unstable mode number and the dashed line shows the limit $\gamma > 0.03\omega_A$.

Figures

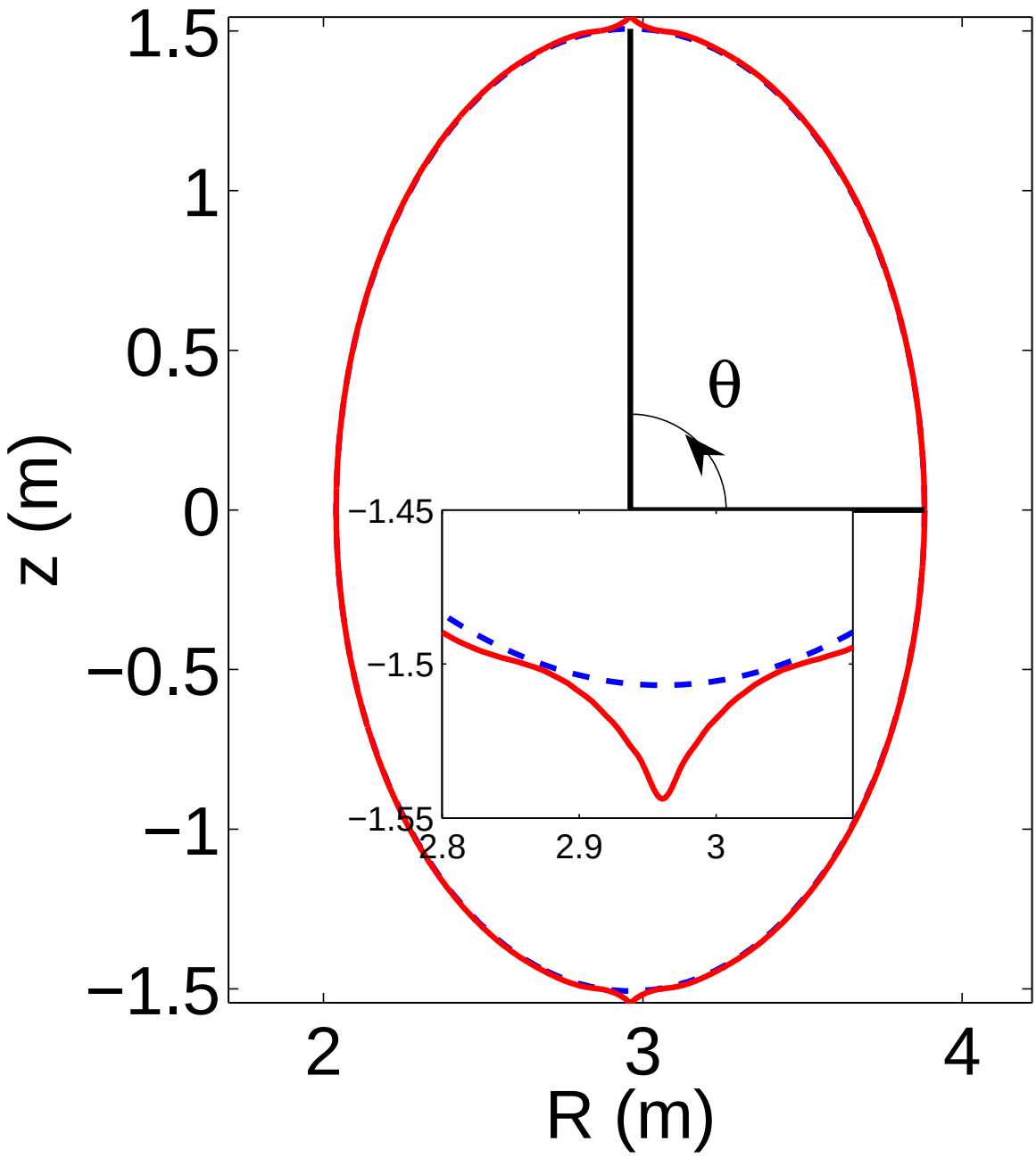

Figure 1. The shape of the last flux surface for the base case equilibrium (dashed line) and steep X-point equilibrium (solid line). The θ angle is used to vary the poloidal location of the X-point.

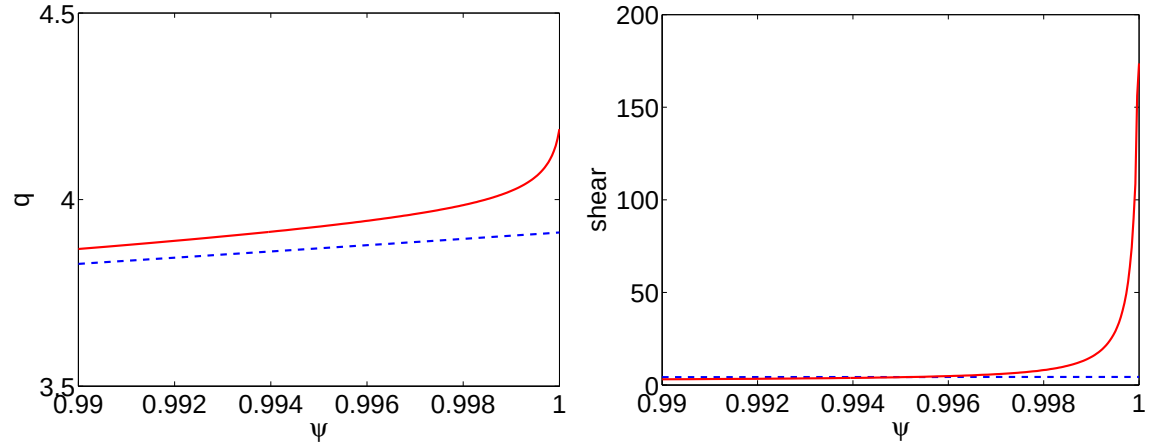

Figure 2. The radial q and magnetic shear profiles of the base case equilibrium (dashed line) and steep X-point equilibrium (solid line) near the plasma edge.

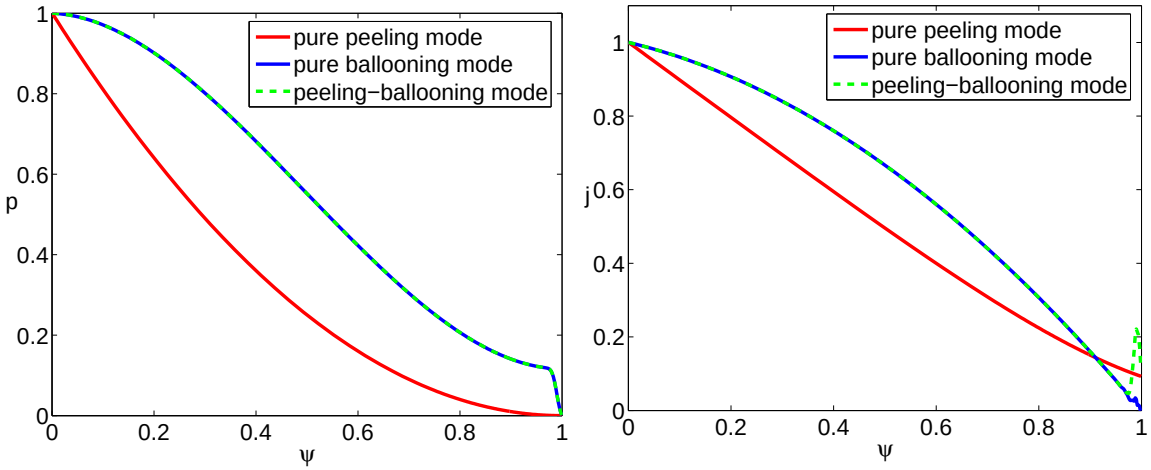

Figure 3. The normalised pressure and toroidal current profiles used for peeling, ballooning and peeling-ballooning modes

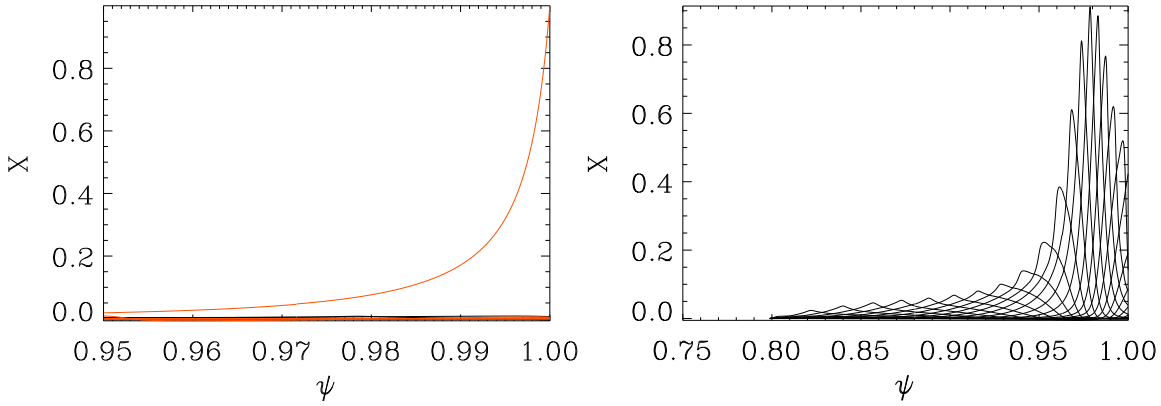

Figure 4. The radial mode structure of $n = 5$ peeling mode (left) and $n = 20$ ballooning mode. X is the radial perturbation of the fluid element. The individual lines represent contributions of different poloidal mode numbers u_m, i.e. the total displacement is $\sum_m u_m(\psi)e^{-im\omega}$.

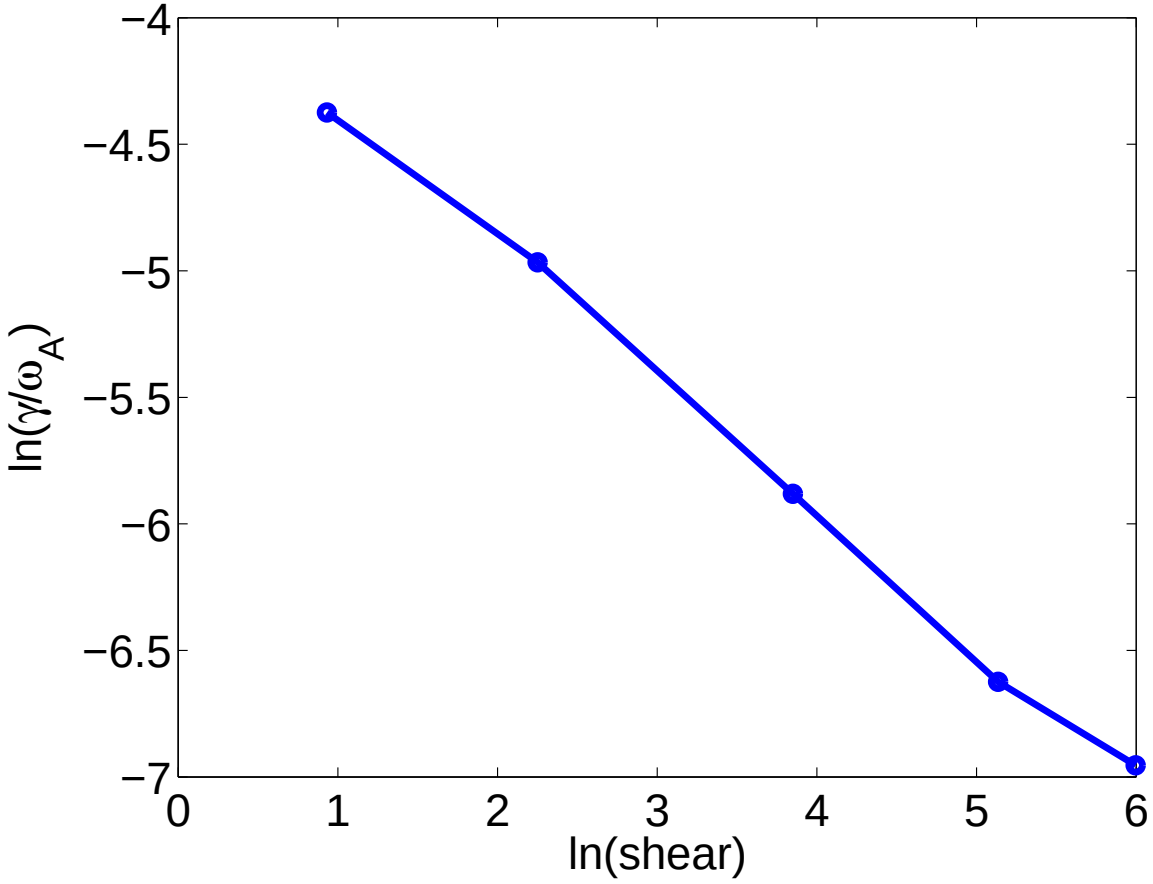

Figure 5. The growth rate of $n = 5$ peeling modes as a function of the edge shear (X-point "sharpness").

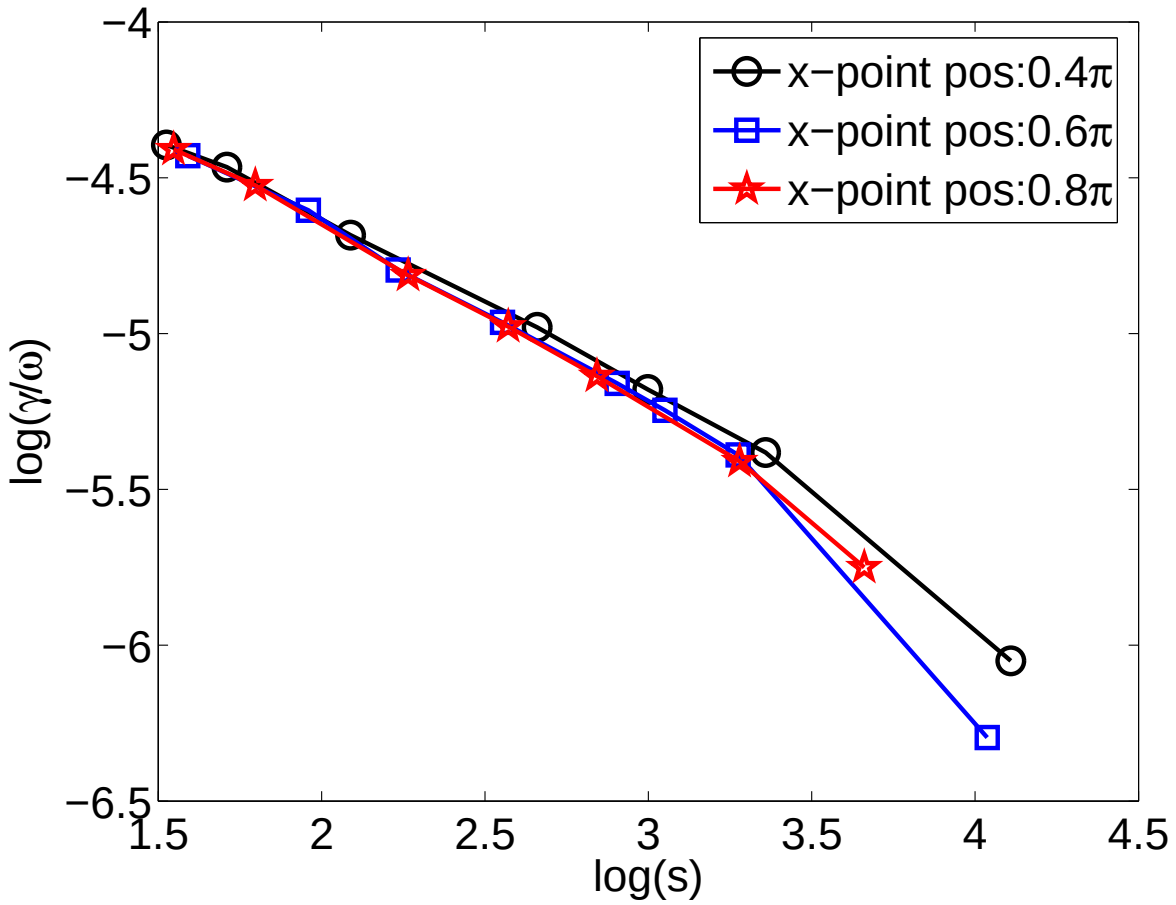

Figure 6. The growth rate of $n = 5$ peeling modes as a function of the edge shear (X-point "sharpness") for three poloidal locations of the X-point.

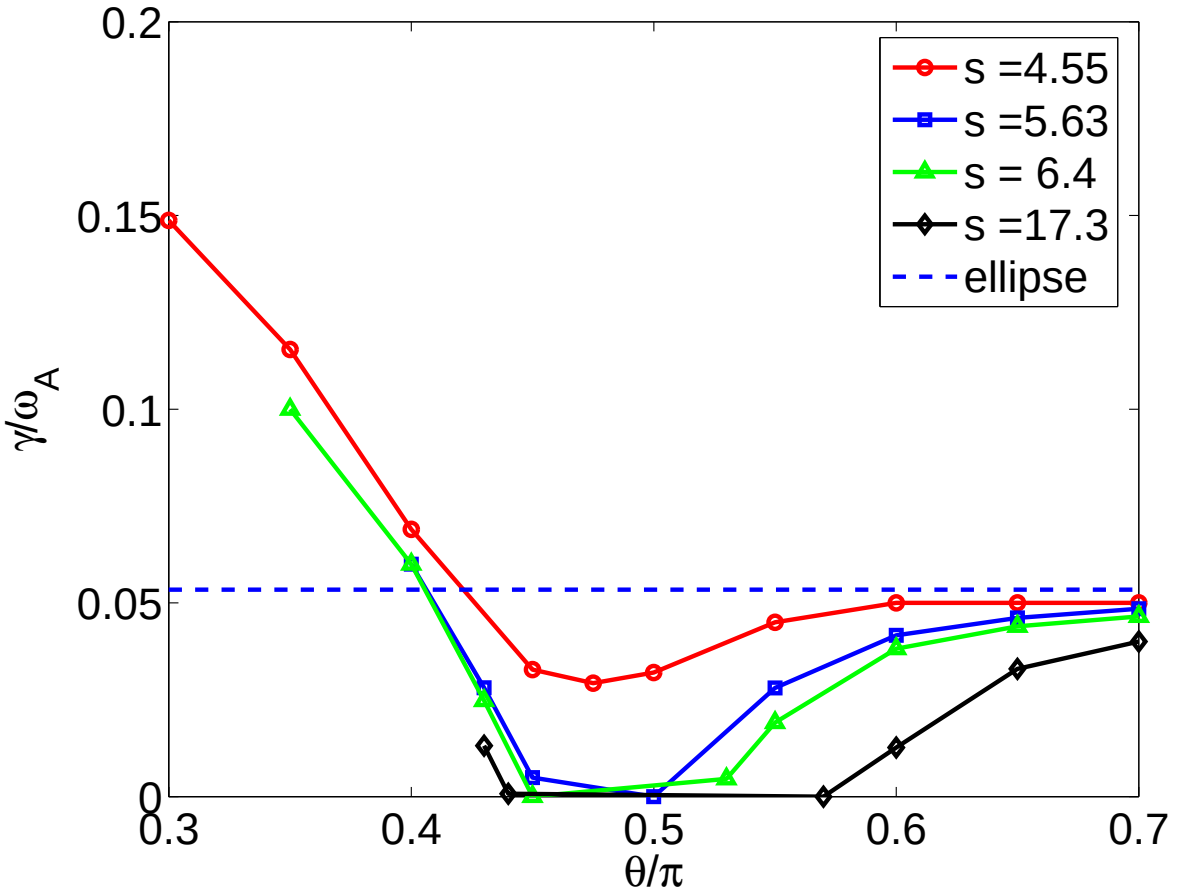

Figure 7. The growth rate of $n = 20$ ballooning mode as a function of the X-point poloidal location for four values of the edge shear.

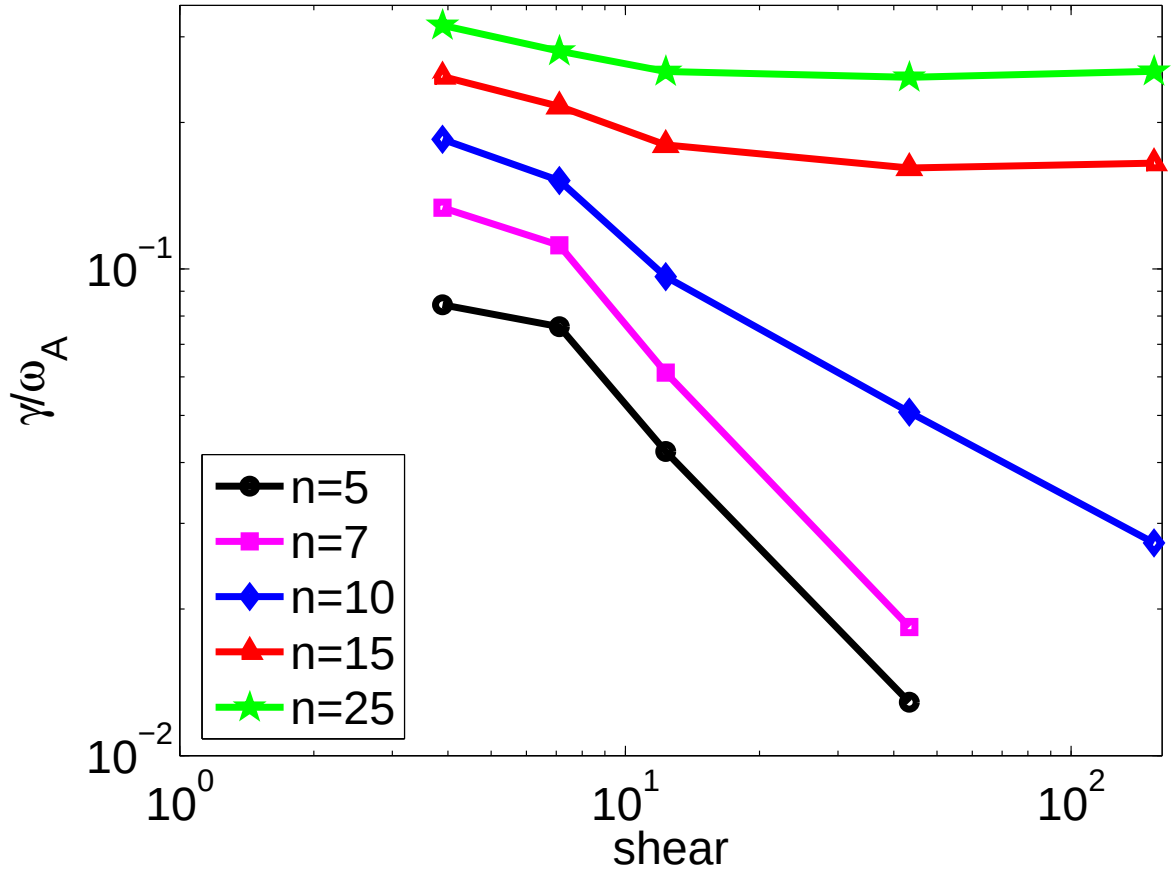

Figure 8. The growth rate of peeling-ballooning modes as a function of the edge shear (X-point "sharpness").

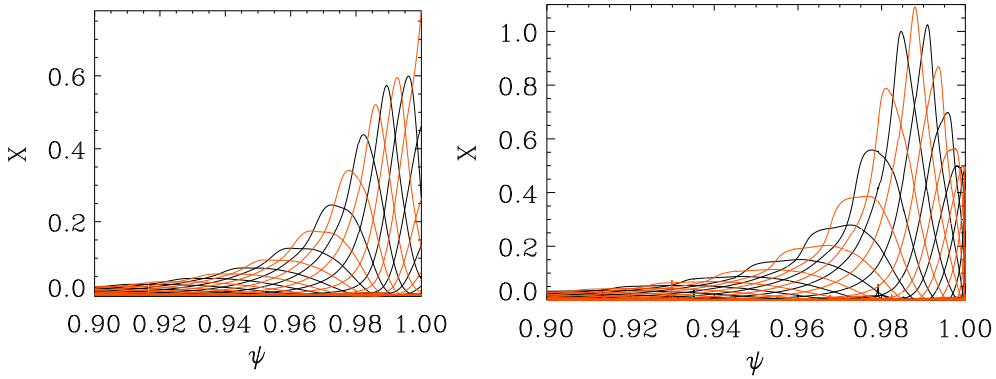

Figure 9. The radial mode structure of n=20 peeling-ballooning mode without (left) and with X-point (right). The X-point case corresponds to the equilibrium with edge shear of 152 in Fig. 8

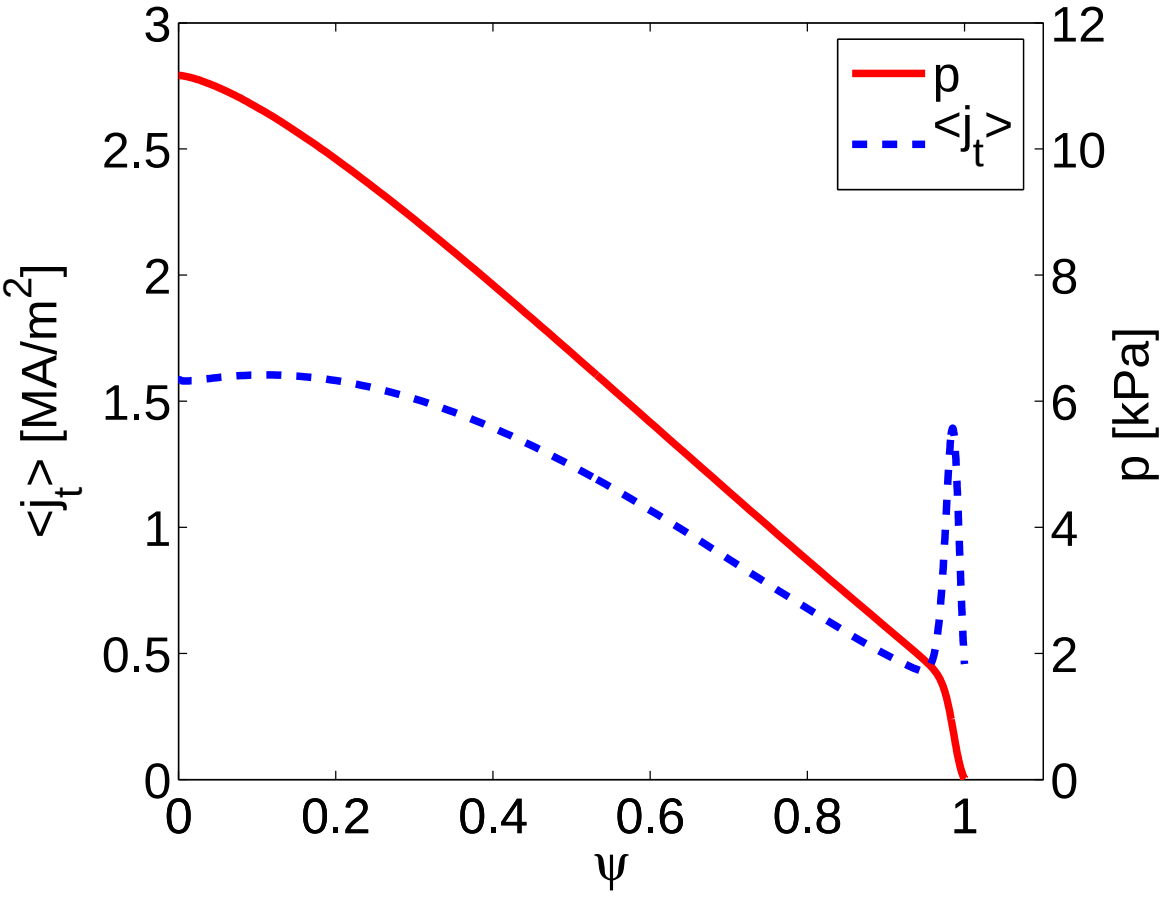

Figure 10. The plasma pressure and flux surface averaged toroidal current profile of MAST discharge #8209.

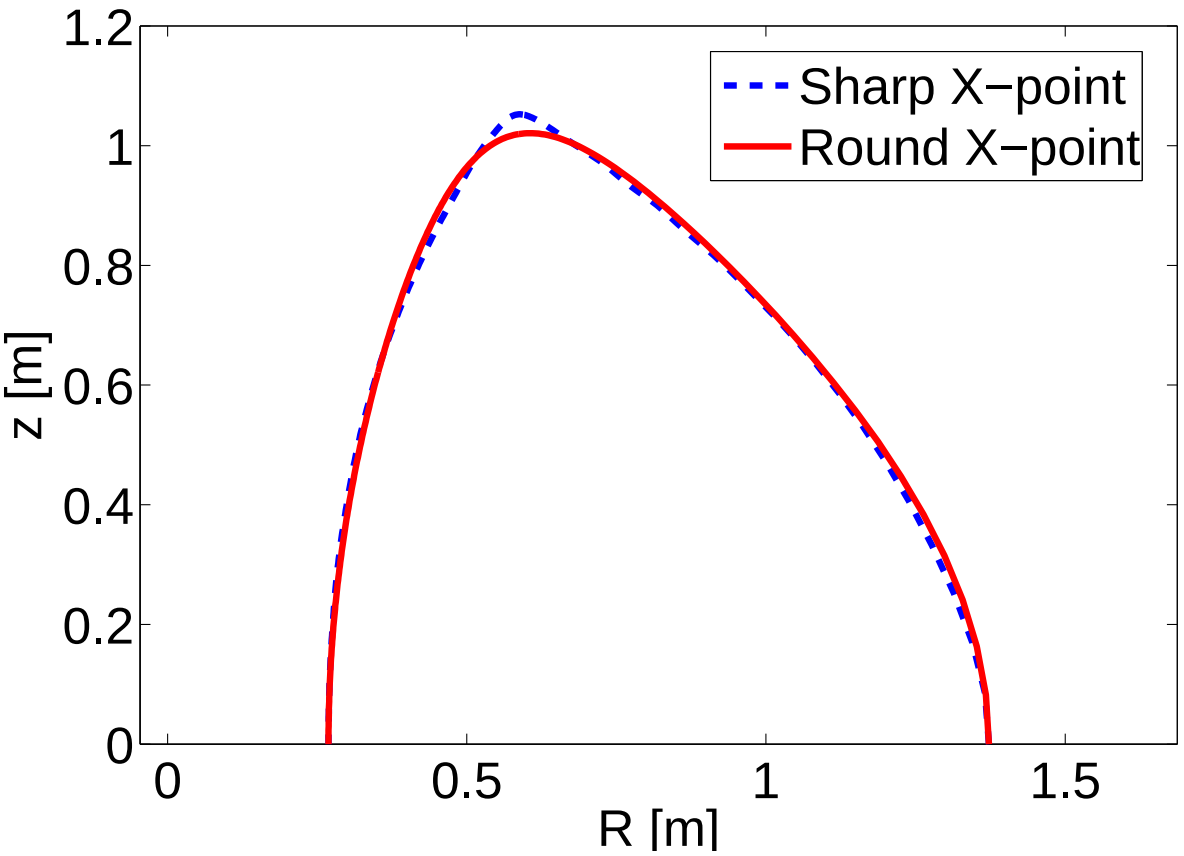

Figure 11. The plasma shape of MAST discharge #8209 with round (dashed line) and sharp (solid line) X-point.

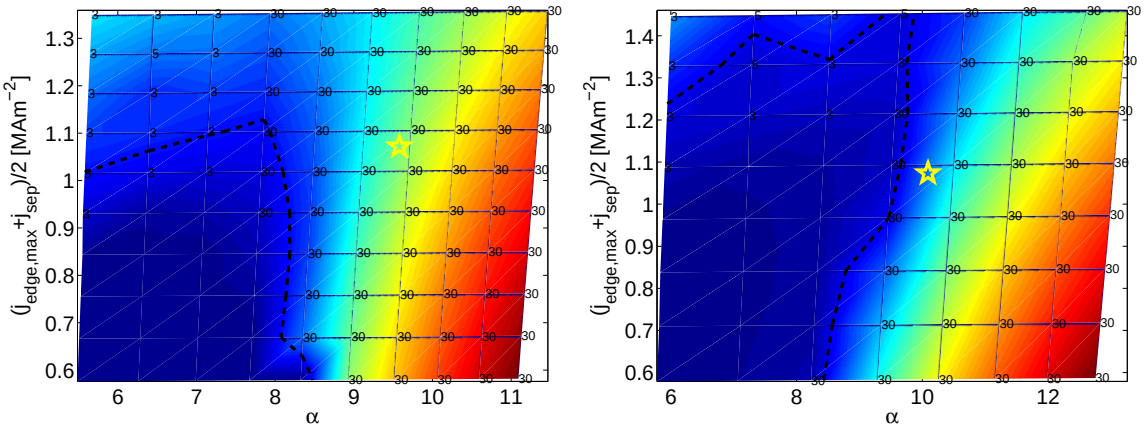

Figure 12. The edge stability diagram for the two plasma shapes of a MAST discharge #8209. The colour represents the growth rate of the mode (dark blue=stable). The left diagram corresponds to a round X-point ($s_{edge} = 8.3$) and the right to a sharp X-point ($s_{edge} = 18.3$). The numbers represent the most unstable mode number and the dashed line shows the limit $\gamma > 0.03\omega_A$.